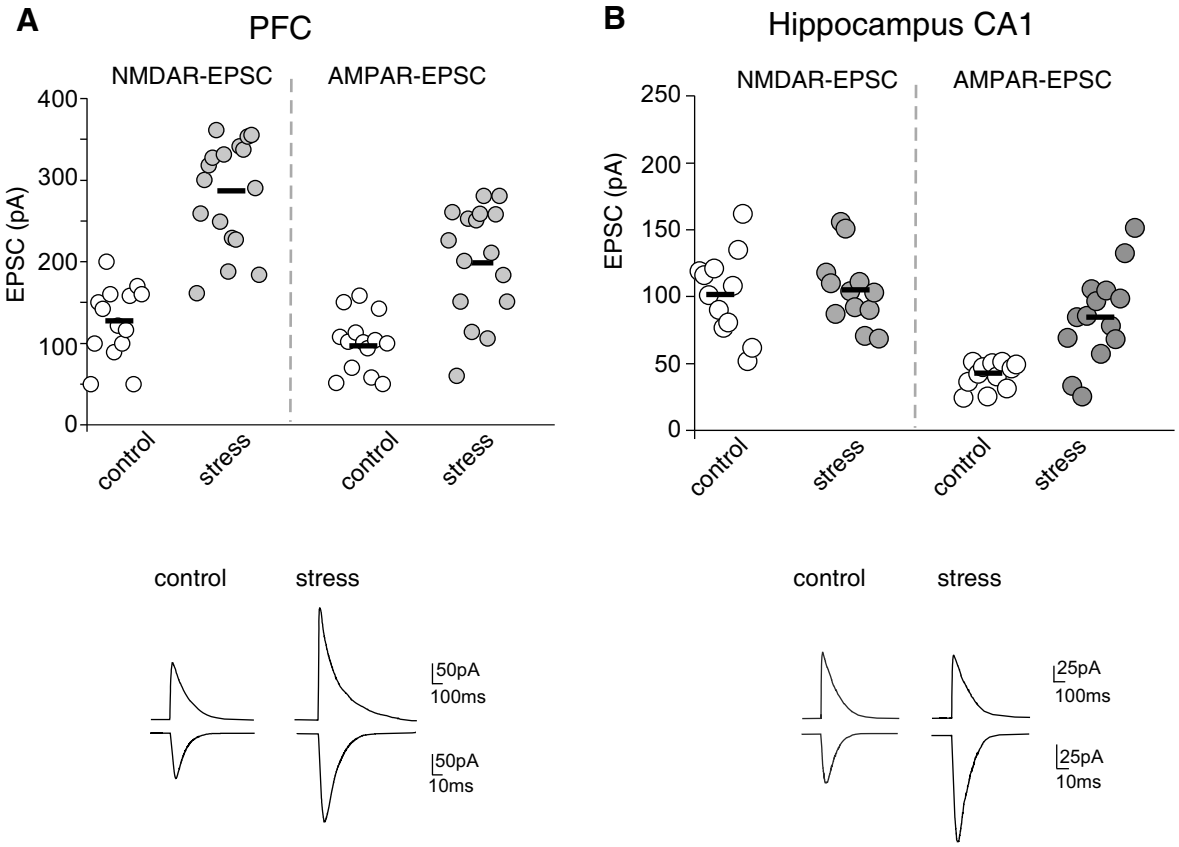

Supplemental Figure 1. Recordings of AMPAR- and NMDAR-mediated EPSCs in the same cells from PFC or hippocampus. Neurons were held at -70 mV to obtain AMPAR-EPSC, followed by +40mV with addition of CNQX (20μM) to record NMDAR-EPSC. Bicuculline (10μM) was present throughout the recording. One neuron per slice was recorded and extensive wash was performed between recordings to prevent contamination of receptor antagonists.
A. In PFC pyramidal neurons, acute stress significantly increased both NMDAR-EPSC (control: 126.2±11.9 pA, n=14; stressed: 282±16 pA, n=17; $p<0.001$, *t* test) and AMPAR-EPSC (control: 100.1±9.2 pA, n=14; stressed: 198.9±16.4 pA, n=17; $p<0.001$, *t* test) to a similar extent. **B.** In CA1 pyramidal neurons, acute stress only increased AMPAR-EPSC significantly (control: 42.0±9.1 pA, n=12; stressed: 85.6±9.2 pA, n=16; $p<0.001$, *t* test), while left NMDAR-EPSC unchanged (control: 102.0±9.1 pA, n=12; stressed: 104±7.8 pA, n=12; $p>0.05$, *t* test).

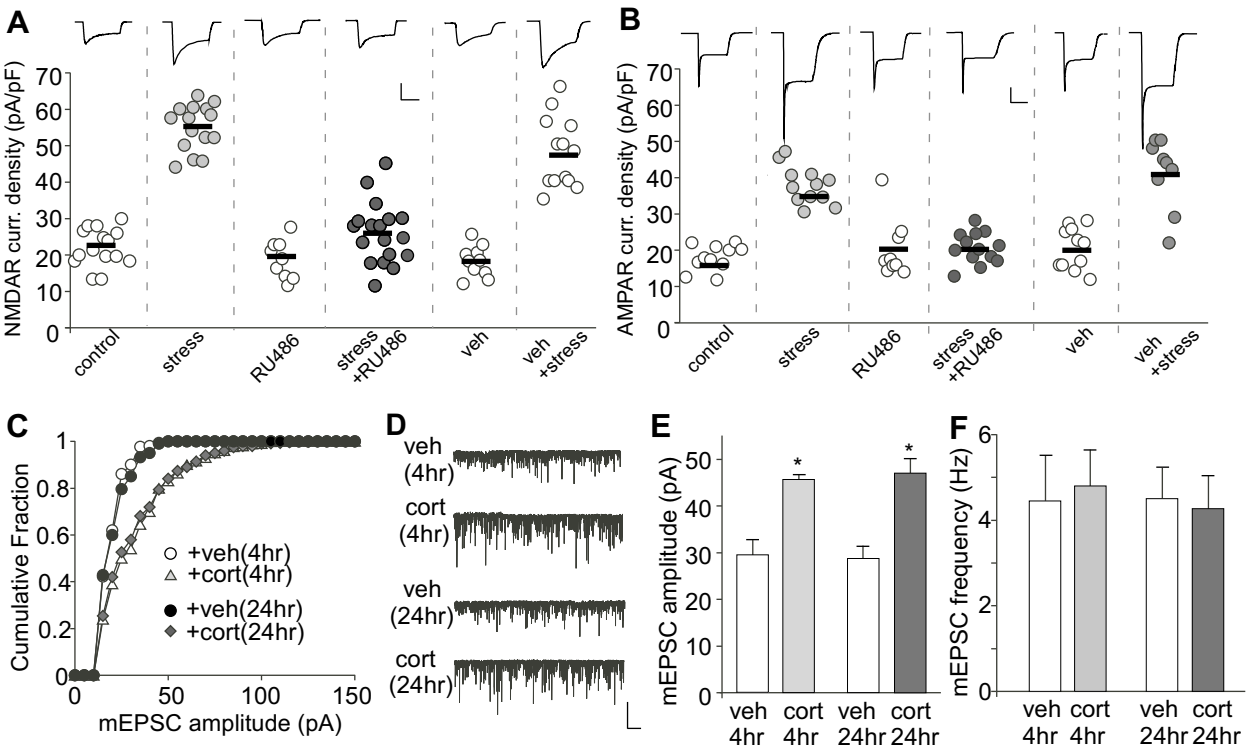

Supplemental Figure 2. AMPAR- and NMDAR-mediated ionic currents and mEPSC after acute stress or corticosterone treatment. A,B. Animals exposed to forced-swim stress had a significantly increased NMDAR and AMPAR current density (pA/pF, NMDA: control: 22.1±1.4, n=15; stressed: 54.9±1.6, n=15; AMPA: control: 16.9±1.1, n=11; stressed: 36.3±1.2, n=12; $p<0.001$, t test), which was abolished by injection (i.p.) of the GR antagonist RU486 (10 mg/kg) (NMDA: RU486: 19.0±1.7, n=9; RU486+stress: 26.2±1.9, n=18; AMPA: RU486: 19.9±2.4, n=10; RU486+stress: 20.5±1.2, n=13; $p>0.05$, t test), but not the vehicle (DMSO) control. **C-F.** The amplitude of mEPSC was significantly increased in PFC cultures at 4 hr or 24 hr after corticosterone treatment (4 hr: vehicle: 29.5±3.2 pA, n=8, cort: 45.6±1.2 pA, n=7; $p<0.001$, *t* test; 24 hr: vehicle: 28.7±2.7 pA, n=8, cort: 47.0±3.2 pA, n=7; $p<0.001$, *t* test). The mEPSC frequency was not altered by corticosterone treatment (4 hr: vehicle: 4.5±1.1 Hz, n=8, cort: 4.8±0.9 Hz, n=7; $p>0.05$, *t* test; 24 hr: vehicle: 4.5±0.7 Hz, n=6, cort: 4.3±0.8 Hz, n=7; $p>0.05$, *t* test).

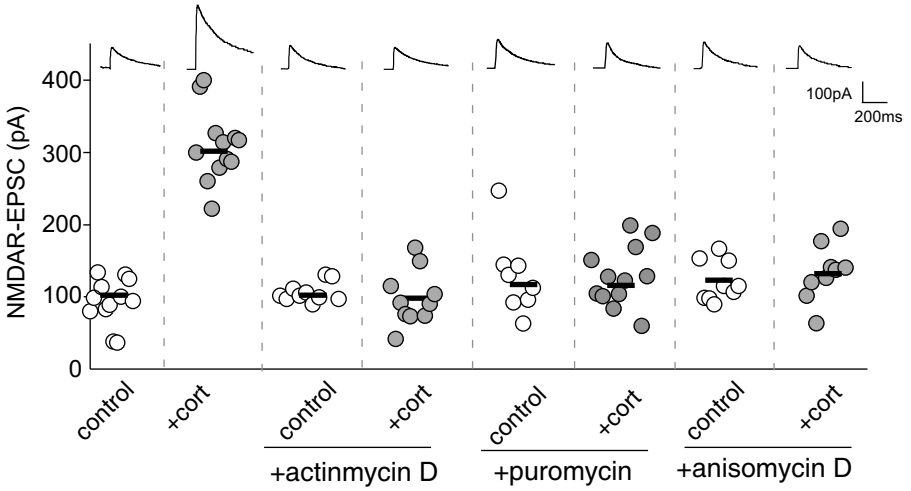

Supplemental Figure 3. The effect of corticosterone on NMDAR-EPSC in the presence of transcription or translation inhibitors. The enhancing effect of corticosterone (100 nM, 20 min) on NMDAR-EPSC in PFC slices (control: 103.5± 11.1 pA, n=15; cort: 309 ± 14.4 pA, n=12; $p<0.001$, t test) was abolished by pre-treatment with the transcription inhibitor actinmycin D (50 μM, 30 min; 96.3 ±11.9 pA, n=10) or puromycin (100 μM, 30 min, 127.5±12.1 pA, n=12). Pre-treatment of PFC slices with translation inhibitor anisomycin D (2 μM, 30 min) also blocked the effect of corticosterone on NMDAR-EPSC (132.2±12.9 pA, n=9).

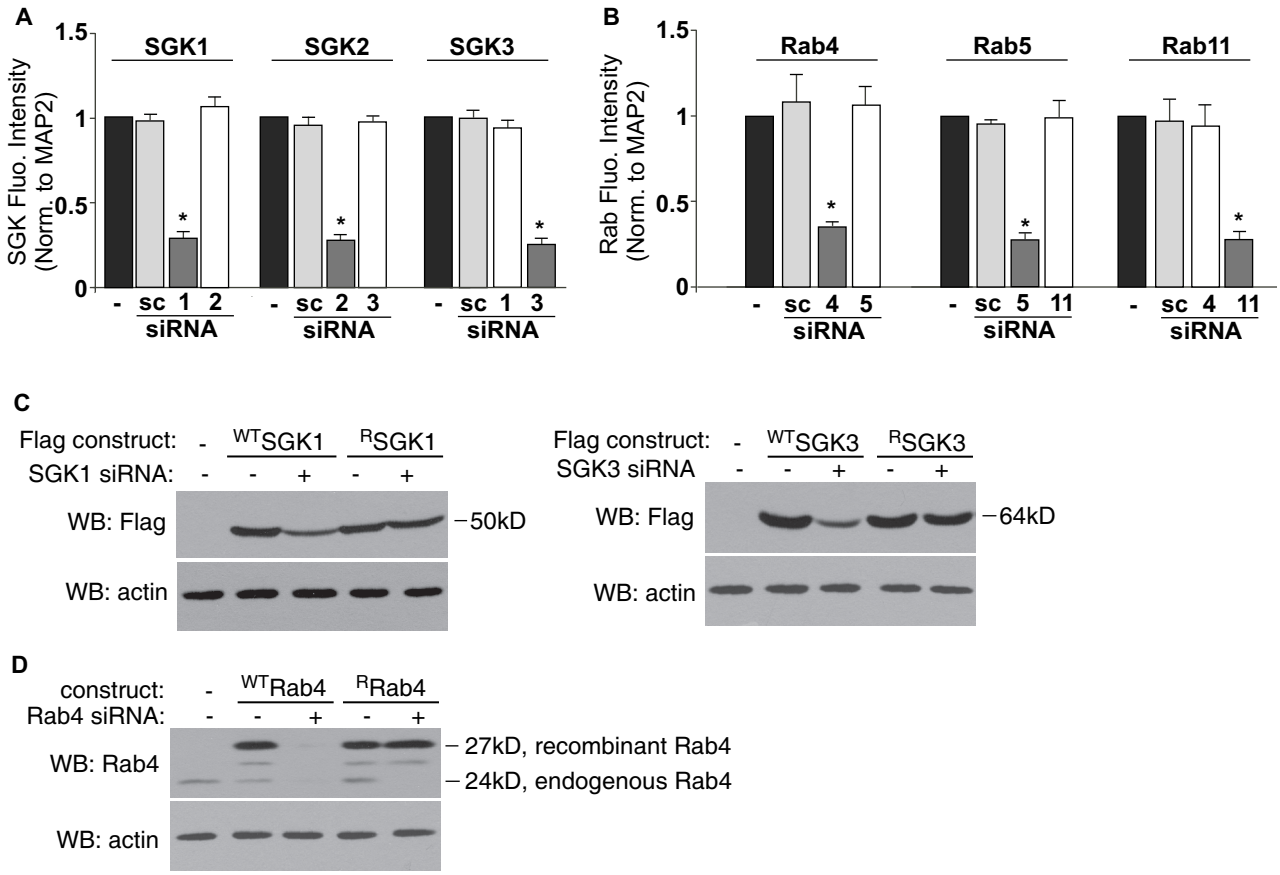

Supplemental Figure 4. Quantification data showing the target-specific gene knockdown by various siRNAs. PFC cultures were transfected with a scrambled control siRNA (sc) or the siRNA against SGK1-3 (A), or Rab4/5/11 (B). GFP was co-transfected. Neurons were co-stained with anti-MAP2 and an antibody against SGK1-3 or Rab4/5/11. The fluorescent intensity (normalized to MAP2) in GFP+ neurons was quantified and compared. **A.** SGK1 was reduced to 0.29±0.04 of control in SGK1 siRNA-transfected cells (n=13), but not altered in cells transfected with scrambled (n=11) or SGK2 siRNA (n=10). SGK2 was reduced to 0.28±0.03 of control in SGK2 siRNA-transfected cells (n=12), but not altered in cells transfected with scrambled (n=10) or SGK3 siRNA (n=14). SGK3 was reduced to 0.27±0.04 of control in SGK3 siRNA-transfected cells (n=13), but was not altered in cells transfected with scrambled (n=10) or SGK1 siRNA (n=13). *: $p<0.001$. **B.** Rab4 was reduced to 0.35±0.03 of control in Rab4 siRNA-transfected cells (n=15), but was not altered in cells transfected with scrambled (n=9) or Rab5 siRNA (n=14). Rab5 was reduced to 0.19±0.02 of control in Rab5 siRNA-transfected cells (n=13), but was not altered in cells transfected with scrambled (n=11) or Rab11 siRNA (n=9). Rab11 was reduced to 0.21±0.04 of control in Rab11 siRNA-transfected cells (n=12), but was not altered in cells transfected with scrambled (n=12) or Rab4 siRNA (n=13). *: $p<0.001$. **C, D.** Representative Western blots in HEK293 cells transfected with wild-type (WT) or siRNA-resistant (R) SGK1, SGK3 (subcloned to pcDNA3.1 vector) or Rab4 (subcloned to plenti6/V5 vector) in the absence or presence of the corresponding siRNA.

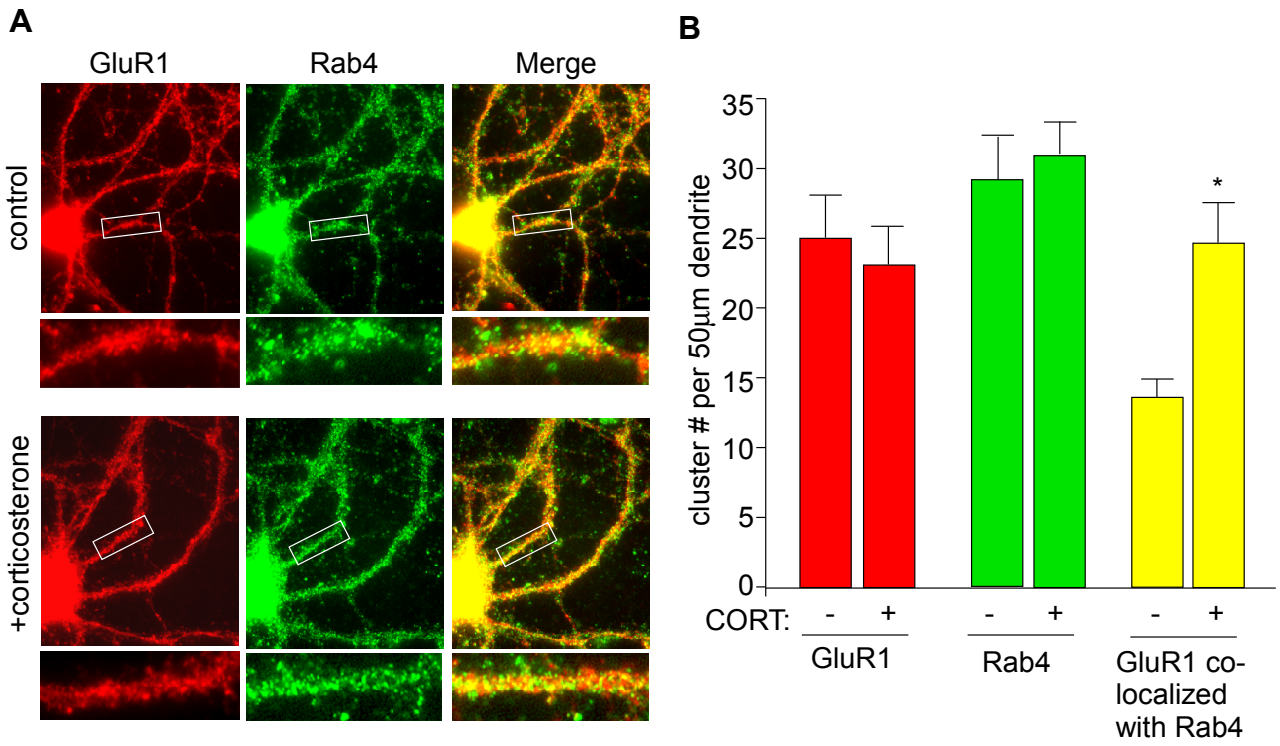

Supplemental Figure 5. Measurement of co-localization of GluR1 and Rab4 in PFC cultures treated with or without corticosterone. **A.** As indicated by yellow puncta along dendrites, AMPA receptors can be seen in Rab4-positive internal vesicles. **B.** Cort-treated neurons show more GluR1 clusters co-localized with Rab4 (control: 13.7±1.4, n=10; CORT: 24.8±2.9, n=10; $p<0.01$, *t* test). No significant changes were found with total GluR1 (control: 25.1±3.4; GluR1-CORT: 23.2±2.7, n=10; $p>0.05$, *t* test) or Rab4 (control: 29.2±3.1; CORT: 31.0±2.3, n=10; $p>0.05$, *t* test).

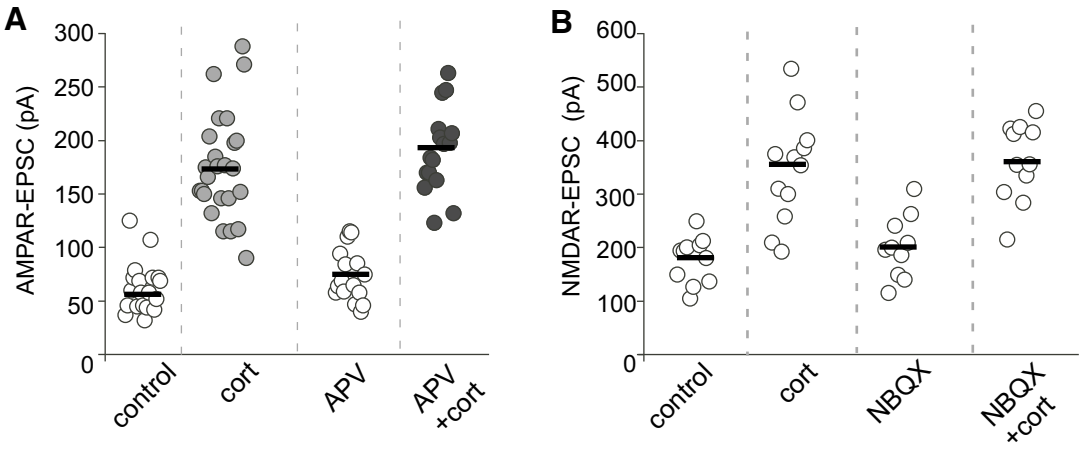

Supplemental Figure 6. The effect of corticosterone on AMPAR-EPSC when NMDAR activation is blocked, and the effect of corticosterone on NMDAR-EPSC when AMPAR activation is blocked. The NMDAR antagonist APV (100 μM) or the AMPAR antagonist NBQX (10 μM) was added 15 min before and during corticosterone treatment (20 min). Recordings were performed at 1-4 hrs after washing off these compounds. **A.** The corticosterone-induced increase of AMPAR-EPSC was not blocked by APV (APV: 73.9±6.1 pA, n=16; APV+cort: 190±9.8 pA, n=16, $p<0.001$, *t* test). **B.** The corticosterone-induced increase of NMDAR-EPSC was not blocked by NBQX (NBQX: 203.3±18.6 pA, n=10; NBQX+cort: 358.1±22.2 pA, n=11, $p<0.001$, *t* test).

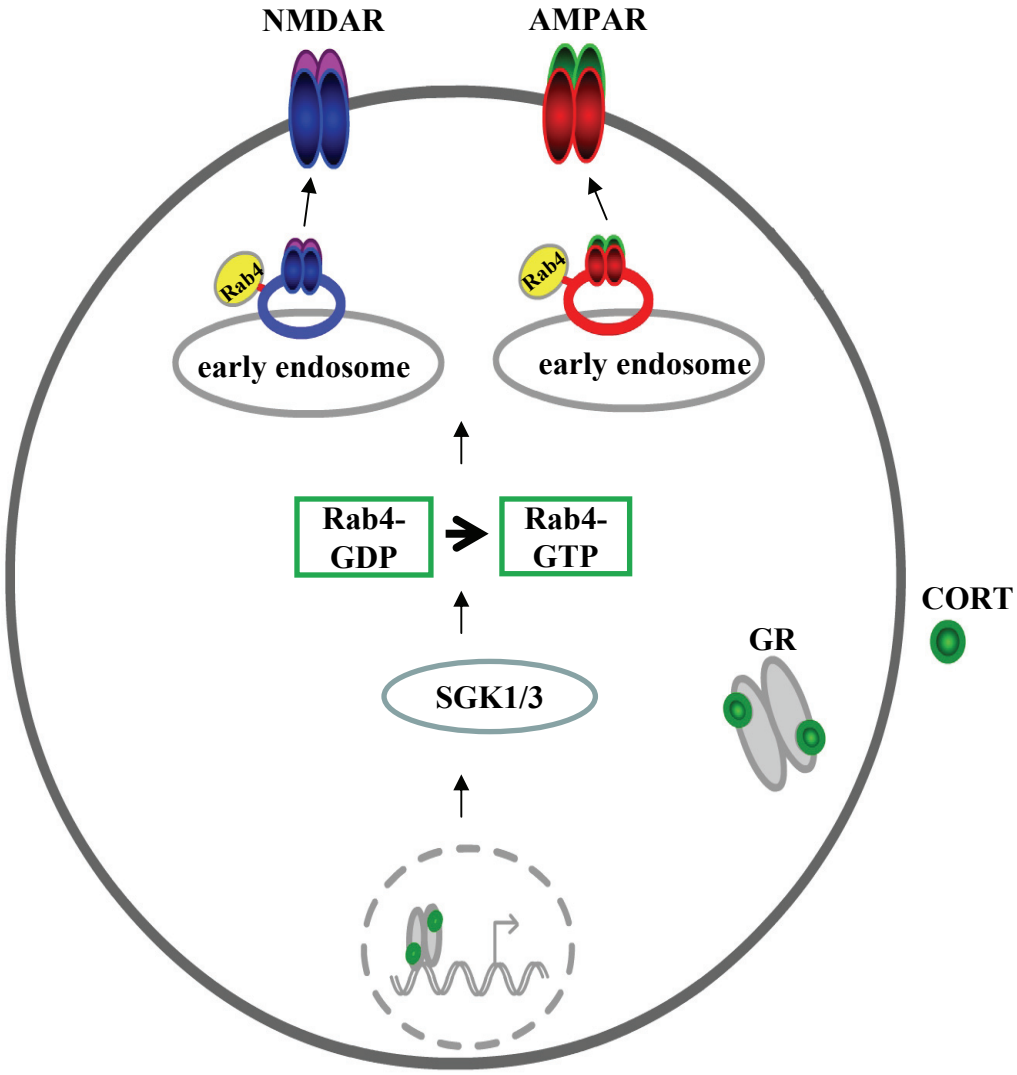

Supplemental Figure 7. A diagram showing the potential molecular and cellular mechanism underlying corticosterone regulation of NMDAR and AMPAR trafficking and function. Upon GR activation, SGK1/3 is upregulated, leading to the activation of Rab4. Consequently, the recycling of NMDARs and AMPARs from early endosome to plasma membrane is enhanced. The extra-synaptic glutamate receptors are moved to synaptic surface presumably via lateral diffusion. At synapses, glutamate receptors are endocytosed for recycling or degradation.